Cocoa shell ingredients improve their lipid-lowering properties under simulated digestion: *In vitro* and HepG2 cells study

Cheyenne Braojos [a,b], Miguel Rebollo-Hernanz [a,b], Silvia Cañas [a,b], Yolanda Aguilera [a,b], Alicia Gil-Ramírez [a,b], Vanesa Benítez [a,b,1], Maria A. Martín-Cabrejas [a,b,*,1]

[a] *Department of Agricultural Chemistry and Food Science, Universidad Autónoma de Madrid, 28049 Madrid, Spain*
[b] *Institute of Food Science Research, CIAL (UAM-CSIC), 28049 Madrid, Spain*

A B S T R A C T

Cocoa (*Theobroma cacao*) shell, the main by-product of cocoa industry, is associated with the regulation of several biomarkers of metabolic syndrome. However, there is little information about the digestion effect on the physiological properties of cocoa shell. The aim of this study was to assess the impact of a standardized *in vitro* digestion protocol on the hypolipidemic capacity of two cocoa shell ingredients, a flour (CSF) and an aqueous extract (CSE), through the evaluation of their *in vitro* hypolipidemic properties and lipid-lowering effects in HepG2 cells. CSF and CSE digested fractions increased their capacity to bind primary bile acids (16–88 %) and inhibit lipase activity (41–100 %), while their ability to bind secondary bile acids (33–42 %) was maintained. Likewise, the digested fractions of cocoa shell ingredients reduced the solubility of the cholesterol micelles (35–97 %) and inhibited the hydroxymethylglutaryl-Co-enzyme A reductase (HMGCR) activity (18–100 %). The hypolipidemic properties of non-digested fractions further enhanced the CSF potential to decrease lipid absorption. Cocoa shell ingredients demonstrated lipid-lowering properties after simulated digestion by effectively reducing the accumulation of intracellular lipids (78–122 %), triacylglycerides (60–90 %), and cholesterol (100 %) induced by palmitic acid in hepatic cells. These results were confirmed by their ability to stimulate lipolysis, reducing the increase in lipase activity (28–78 %) and increasing glycerol release (27–80 %) with respect to palmitic acid treated cells, and inhibiting HMGCR activity. Phenolic compounds and dietary fiber are significantly associated to the observed hypolipidemic effects of cocoa shell ingredients. These findings demonstrated the potential efficacy of CSF and CSE in reducing lipid absorption and reversing its hepatic accumulation. Hence, these cocoa shell ingredients might prevent diseases related to lipid accumulation by improving overall health status.

1. Introduction

Cocoa (*Theobroma cacao*) is one of the most consumed ingredients worldwide, approximately 5.0 million tons annually, and its production continues rising (Panak Balentić et al., 2018). After harvesting, cocoa beans are extracted from their pods, fermented, dried, and conducted to chocolate manufacturing facilities (Rojo-Poveda et al., 2020). Throughout this process, about 90 % of cocoa bean is turned into by-products, which represent an economic and environmental issue (Mariatti et al., 2021). In particular, the cocoa shell, also known as husk or hull, is the main cocoa by-product generated during the roasting of cocoa beans, accounting for 700,000 tons per year (Cantele et al., 2020).

The cocoa shell chemical composition varies depending on genetics and climatic conditions, among others. In general, it is characterized by abundant carbohydrates (62 %), and proteins (12–22 %), and a variable lipid content (2–18 %) (Panak Balentić et al., 2018). Its composition also includes the presence of dietary fiber (39–66 %) and valuable bioactive compounds, such as theobromine, caffeine and phenolic compounds, associated with the regulation of metabolic syndrome biomarkers, such as lipid accumulation, inflammation, oxidative stress, hypertension and insulin resistance (Cinar et al., 2021; Rebollo-Hernanz et al., 2022; Ruvira et al., 2023).

A chronic lipid accumulation may lead to atherosclerosis, type 2 diabetes, obesity and non-alcoholic fatty liver disease (NAFLD) (Li et al.,

2019). Recent studies have accomplished those functional foods or extracts rich in (poly)phenols protect against the development and progression of NAFLD in animals and reduce its clinical symptoms in humans (Noori et al., 2017; Tan et al., 2017; Yassin Zamanian et al., 2023). Currently, a potential intervention window for reducing lipid accumulation is the alteration of fat digestion and absorption with the possible impact on lipid and lipoprotein metabolism (Ko et al., 2020). Lipid digestion primarily occurs in the small intestine, although a minor portion is processed in the stomach by gastric lipase. Fats stimulate the release of bile salts, which emulsify lipids and promote the action of the pancreatic lipase, breaking down fats into glycerol, monoglycerides, and fatty acids, which form micelles for their absorption by enterocytes (Li et al., 2019). Lately, we have demonstrated the cocoa shell may alter the lipid digestion and absorption due to its *in vitro* ability to bind bile salts and cholesterol, and to inhibit the lipase activity (Benítez et al., 2023). Moreover, we have proven the capacity of the cocoa shell phytochemicals to prevent NAFLD *in vitro* (Rebollo-Hernanz et al., 2022).

The promising hypolipidemic properties of cocoa shell and its sensory characteristics comparable to chocolate allow its use as a potential functional ingredient (Nogueira Soares Souza et al., 2022). However, there is little information on the impact of digestion on cocoa shell bioactive compounds and their biological function, which is crucial to maximize the potential of cocoa shell as a bioactive food ingredient for the prevention of lipid accumulation-related diseases. Presently, *in vitro* static digestion is used as a valuable research tool to predict and understand the possible effects that the digestion process may have on food properties. This methodology is widely accepted in food and nutritional sciences as a feasible, reproducible, flexible, and easy first approach to simulate digestion under physiological conditions (Brodkorb et al., 2019). Hence, the aim of this study was to assess the impact of a standardized *in vitro* digestion protocol (INFOGEST) on the hypolipidemic capacity of two cocoa shell ingredients, a flour and an aqueous extract, to understand their potential in the prevention of diseases related to lipid accumulation. To achieve this objective, the *in vitro* hypolipidemic properties and lipid-lowering effects in HepG2 cells of these cocoa shell ingredients were evaluated.

2. Materials and methods

2.1. Materials

Dulbecco's Modified Eagle Medium low glucose (1000 mg mL^{-1}) (DMEM) and 0.25 % trypsin-EDTA were obtained from GE Healthcare Life Sciences. Fetal Bovine Serum (FBS) and penicillin–streptomycin (100×) were acquired from Gibco Life Technologies (Waltham, MA USA). *o*-Phthalaldehyde, furfural, bile salts, lipase, Tween® 20, Pepsin (P7012), Pancreatin (P7545), Pronase E, Viscozyme, Bovine Serum Albumin (BSA), Palmitic Acid (PA), 2′,7′-Dichlorofluorescein diacetate (DCFDA), Bradford Reagent and Oil Red O were purchased from Sigma-Aldrich (St. Louis, MO, USA). 3-(4,5-Dimethylthiazol-2-yl)-5-(3-carboxymethoxyphenyl)-2-(4-sulfophenyl)-2H-tetrazolium (MTS) was purchased from Promega Corporation (Carlsbad, CA, USA). All other chemicals and reagents were obtained from Panreac (Barcelona, Spain) unless otherwise specified.

2.2. Cocoa shell flour and aqueous extract preparation

The cocoa shell was provided by Chocolates Santocildes (Castrocontrigo, León, Spain). The cocoa shell flour (CSF) was obtained after milling in a pilot scale ball mill (Ortoalresa-Álvarez Redondo S.A., Madrid, Spain) for 72 h and the cocoa shell aqueous extract (CSE) as described by Rebollo-Hernanz et al. (2019). Briefly, the CSF (0.02 g mL^{-1} solid- to solvent ratio) was added to boiling water 100 °C and stirred for 90 min. After extraction the aqueous extract was filtered, frozen at −20 °C, and freeze-dried. Both ingredients were stored at −20 °C until use.

2.3. Static in vitro simulated digestion

Static *in vitro* simulated gastrointestinal digestion was carried out according to the INFOGEST protocol with slightly modifications (Brodkorb et al., 2019). Briefly, to simulate the oral phase, CSF (1 g) or CSE (100 mg) was mixed with simulated salivary fluid (SSF) and the mixture was kept for stirring (2 min, 37 °C, pH 7). The gastric phase was performed by combining the oral phase with simulated gastric fluid (SGF) and adding porcine pepsin solution (2000 U mL^{-1} digestion), the resulted samples were incubated under agitation (2 h, 37 °C, pH 3). To simulate the intestinal phase, the gastric phase was mixed with simulated intestinal fluid (SIF) containing pancreatin (100 U trypsin activity mL^{-1} digestion) and samples were incubated under agitation (2 h, 37 °C, pH 7) The static *in vitro* simulated colonic digestion was performed following the method previously described by Papillo et al. (2014). Pronase E (5 mL, 1 mg mL^{-1}) was added to the intestinal phase, and the pH was adjusted to 8.0. The samples were incubated under stirring (1 h, 37 °C). After, pH was adjusted to 4, Viscozyme (150 μL) was added, and samples were incubated (16 h, 37 °C) under agitation. A digestion blank was prepared for each digestion phase containing the simulated digestion fluids. After centrifugation (800×*g*, 5 min), the supernatants of each phase (digested fractions) were collected, lyophilized, and redissolved in phosphate buffer saline (PBS) (0.1 mol L^{-1}, pH 7.2). The pellets (non-digested fractions) were freeze-dried and stored at −20 °C until further use. Both digested and non-digested fractions were obtained within each digestion phase in the CSF, whereas, in the CSE, only the digested fractions were generated and collected (Fig. 1).

2.4. Chemical characterization

A Truspec 630–200-200 elemental analyzer (St. Joseph, MI, USA) with a thermal conductivity detector was utilized to determine the total nitrogen content, used to estimate the protein content. Carbohydrate composition was evaluated as previously described Fernandes et al. (2019). The phenolic compounds (TPC) were extracted and measured using the Folin–Ciocalteu method adapted to a microplate protocol, expressing the results as mg gallic acid equivalents per gram (mg GAE g^{-1}) (Cañas et al., 2023). Phenolic compounds and methylxanthines profile were assessed according to Cañas et al. (2022) by a HPLC-DAD (Agilent Technologies, Palo Alto, CA, USA) linked to an API-3200 Qtrap (Applied Biosystems, Darmstadt, Germany) equipped with an ESI source, triple quadrupole-ion trap mass analyzer, and Analyst 5.1 software. The mobile phases utilized were 0.1 % formic acid in water (solvent A) and 100 % acetonitrile (solvent B). The elution gradient employed was isocratic 15 % B for 5 min, 15–20 % B for 5 min, 20–25 % B for 10 min, 25–35 % B for 10 min, 35–50 % B for 10 min, and column re-equilibration. The chromatographic separation of phytochemicals was conducted at a flow rate of 0.5 mL min^{-1} at 35 °C in a Spherisorb S3 ODS-2 C8 column (Waters, Milford, MA, USA) (3 μm, 150 mm × 4.6 mm i.d.).

2.5. Fat-binding capacity

The capacity of the CSF and the CSE to bind fats under digestion conditions were determined as described Zhou et al. (2006) with slight modifications. To simulate gastric conditions, CSF or CSE (0.1 g) were mixed with SGF (2 mL) containing pepsin (2000 U mL^{-1}) and lipase (3850 U activity mL^{-1}) and olive oil was added in increasing concentrations. The mixtures were incubated in agitation (2 h, 37 °C). Later, to simulate intestinal conditions, SIF (4 mL) containing pancreatin (30 U trypsin activity) were added to each mixture and incubated in agitation (2 h, 37 °C). After centrifugation (800×*g*, 15 min), the non-adsorbed oil was collected from the supernatant. The fat-binding capacity was expressed as grams of bound oil per gram of cocoa shell. The maximum amount of adsorbed fat was calculated by obtaining the (second-order) curve's maximum.
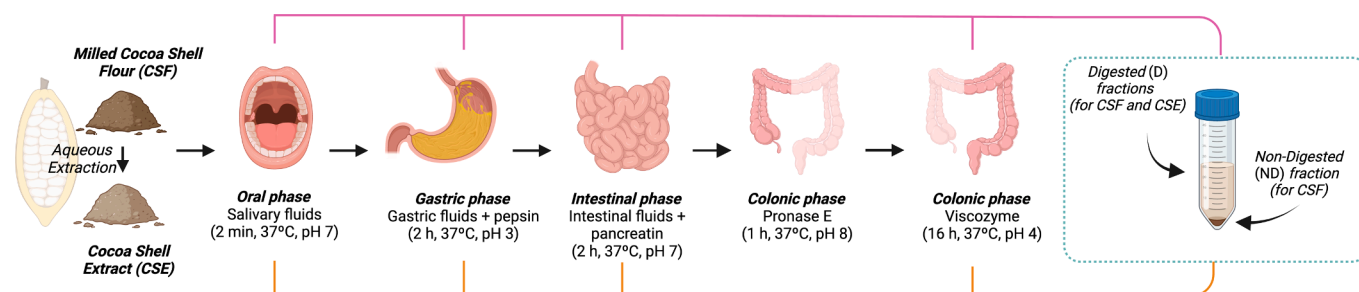
Fig. 1. An illustrative diagram of the simulated digestion process of the cocoa shell flour (CSF) and aqueous extract (CSE).

2.6. In vitro hypolipidemic properties of the digested fractions

2.6.1. Reduction of micellar cholesterol solubility capacity

The method described by Vásquez-Villanueva et al. (2019), with slight modifications, was used to evaluate the ability of CS digested fractions to reduce the micellar cholesterol solubility (RMCS). To create the micelles, a mixture of phosphatidylcholine (2.4 mmol L^{-1}), cholesterol (0.5 mmol L^{-1}), and oleic acid (1 mmol L^{-1}) in methanol was dried under nitrogen and redissolved in PBS solution (15 mmol L^{-1}, pH 7.4) with sodium chloride (132 mmol L^{-1}) and taurocholate (6.6 mmol L^{-1}), sonicated (1 min, 20 % amplitude, Branson, 450 Digital Sonifier) and incubated in agitation overnight (37 °C). For the assay, 150 μL of the digested fractions were mixed with 150 μL of the micelle solution. The mixtures were incubated (2 h, 37 °C) and centrifuged (6000×g, 10 min). The supernatants (0.1 mL) were mixed with acetic acid, H_2SO_4 (96 %), and o-phthalaldehyde (0.6 mg mL^{-1}) and incubated (30 min, 60 °C) until color development. The absorbance was measured at 550 nm using a microplate reader to determine the cholesterol staying in the micelles. The RMCS was calculated using the following equation:

$$RMCS\ (\%) = \left(\frac{C_i - C_e}{C_i}\right) \times 100$$

where C_i is the initial concentration of cholesterol in the micelles and C_e is the concentration of cholesterol in the micelles after incubation with the sample.

2.6.2. Capacity to bind primary bile acids

To evaluate the capacity of the CSF and CSE digested fractions to bind bile acid, the method of Ontawong et al. (2019) was followed with slight modifications. Samples (10 mg mL^{-1}) were incubated for 2 h, 37 °C with or without sodium cholate acid (2 mmol L^{-1}, pH 7.0) and centrifuged (1000×g, 15 min). Then, the supernatant (100 μL) was mixed with H_2SO_4 (0.6 mL, 45 % v/v) and furfural (100 μL, 0.3 %) and incubated with agitation (30 min, 65 °C) measuring absorbance at 620 nm.

2.6.3. Capacity to bind secondary bile acids

The capacity of CSF and the CSE digested fractions to bind secondary bile acids was determined as described Levin et al. (1961). The sample (10 mg mL^{-1}) were incubated with or without taurodeoxycholic acid (20 mmol L^{-1}) (2 h, 37 °C) and centrifuged (1000 × g, 10 min). The supernatant (100 μL) was mixed with a fresh solution (10:4:1, H_2SO_4: 85 % orthophosphoric acid:water + redistilled benzaldehyde 1 %) and incubated (1 min, 37 °C). The reaction was stopped with ice and cold ethyl acetate (400 μL) was added. Finally, when two phases were observed, the samples were thoroughly mixed and allowed to stand (25 min), measuring the absorbance at 660 nm.

2.6.4. Pancreatic lipase activity inhibition

The in vitro ability of the CSF and CSE digested fractions to inhibit pancreatic lipase activity was assessed according to Herrera et al. (2018) with slight modifications, using an enzyme kit adapted to a micromethod (Spinreact, Barcelona, Spain). The digested fractions (1 mg mL^{-1}) were mixed with a solution of pancreatic lipase (1 mg mL^{-1} of Tris-HCl 40 mmol L^{-1}, pH 8.3), and the protocol was carried out following the manufacturer's instructions.

2.6.5. Hydroxymethylglutaryl-Co-enzyme A reductase activity inhibition

The capacity of the CSF and CSE digested fractions to inhibit the hydroxymethylglutaryl-Co-enzyme A reductase (HMGCR) activity was measured using the commercial HMGCR Assay kit (Sigma, Madrid, Spain) according to the manufacturer's instructions in a microplate reader (Cytation 5, Biotek, Winooski, VT, USA). Pravastatin (Kern Pharma, Barcelona, Spain) was used as statin positive control of inhibition.

2.7. In vitro hypolipidemic properties of the non-digested fractions

2.7.1. Capacity to bind cholesterol

The capacity to bind cholesterol was evaluated following the method described by Benítez et al. (2023). Briefly, fresh egg yolks were diluted 1:10 (v/w), and the dilution was emulsified, divided, and adjusted to pH 2.0 or 7.0. Samples (0.1 g) and the pH 2 or 7 diluted egg yolk (2 mL) were mixed, incubated in agitation (2 h, 37 °C), and centrifuged (800×g, 15 min). Consecutively, supernatants (0.1 mL) pure acetic acid (0.6 mL), H_2SO_4 (0.2 mL, 96 %) and of o-phthalaldehyde (0,1 mL, 0.6 mg mL^{-1}) were mixed and incubated (30 min, 60 °C) for color development. Finally, absorbance at 550 nm was assessed in triplicate using a microplate reader (Cytation 5, Biotek, Winooski, VT, USA).

2.7.2. Capacity to bind bile salts

The bile-salts binding capacity was determined according to Benítez et al. (2023). Sample (0.1 g) was mixed with a solution of NaCl (0.15 mol L^{-1}, pH 7.0) and sodium cholate (4.65 mmol L^{-1}), incubated (3 h, 37 °C) and centrifuged (800×g, 15 min). Hereafter, supernatant (0.1 mL), H_2SO_4 (45 % v/v) (0.6 mL) and of furfural (0.3 %) (0.1 mL) were incubated in agitation (30 min, 65 °C) for color development. The absorbance was determined by triplicate at 620 nm.

2.7.3. Pancreatic lipase inhibitory activity

The capacity of the CSF non-digested fractions to inhibit the pancreatic lipase activity was measured following the method of Benítez et al. (2021). Sample (0.1 g) was added to mixture of olive oil (2 mL), lipase (0.75 mg mL^{-1} of PBS), and PBS (0.1 mol L^{-1}, pH 7.2) and incubated (1 h, 37 °C). The reaction was stopped in ice (5 min), and then centrifuged (800×g, 15 min). Supernatants were emulsified adding Tween® 20 (0.2 mL). Finally, the lipase activity of each sample was evaluated by a titration with NaOH (0.02 mol L^{-1}). A similar method adding bile salts (15.65 mg mL^{-1}) to the initial mixture was carried out to investigate the effect of bile salts on the lipase inhibition. Lipase inhibitory activity is defined as the percentage of decrease in the free fatty acid production rate over the control.

2.8. Evaluation of the digested fractions lipid-lowering capacity in HepG2 cells

2.8.1. Cell culture

HepG2, human hepatocyte cells, obtained from ATCC (Manassas, VA, USA), were cultured in DMEM (1 g mL^{-1} glucose) containing FBS (10 %) and penicillin/streptomycin (1 %), at 37 °C and 5 % CO$_2$ using a humidified incubator (BINDER CB series 2010, Tuttlingen, Germany). Cell seeding density was 10^5 cells cm^{-2}.

2.8.2. Intracellular fat accumulation induction in HepG2 cells

Intracellular fat accumulation was induced in HepG2 cells, 24 h after seeding, with palmitic acid (PA) (500 μmol L^{-1}, 24 h, 37 °C) in a humidified atmosphere. To prepare the PA solution, PA was conjugated with DMEM containing BSA (1 %).

2.8.3. CSF and CSE digested fractions preparation for HepG2 cells treatment

Samples were diluted in Dulbecco's Phosphate Buffered Saline with calcium and magnesium (DPBS) (0.1 mol L^{-1}) (Cytiva, South Loga, Utah, USA), filtered with 0.45 μm cellulose acetate filters and kept at −80 °C until further analysis.

2.8.4. Experimental design for the prevention of lipid accumulation

After 24 h of seeding, cells were cotreated with CSF or CSE digested fractions (200 μg mL^{-1}) in the presence of PA (500 μmol L^{-1}) for 24 h in a humidified atmosphere. Non-treated cells (NT) were only treated with BSA (1 %). Cell medium was collected, centrifuged, and stored at −80 °C until further analysis. Cells were rinsed twice and lysed with ice-cold PBS (0.1 mol L^{-1}) (Cytiva, South Loga, Utah, USA). The cell suspension was sonicated (24 s, 10 % amplitude, 450 Digital Sonifier, Branson, Brookfield, CT, USA), and centrifuged (10,000×g, 10 min, 4 °C) to remove any cell debris. Supernatants were collected and stored at −80 °C until further analysis. The Bradford method was used for the total proteins' quantification in the cell lysates, using BSA as the standard.

2.8.5. Cell viability

To determine viability, HepG2 cells were grown in 96-well plates and treated as mentioned in section 2.8.4. Viability was measured colorimetrically using the CellTiter 96® AQueous MTS Reagent Powder (Promega Corporation, Madison, WI, USA) following the manufacturer's instructions. The absorbance was read at 490 nm using a microplate reader (Cytation 5, Biotek, Winooski, VT, USA).

2.8.6. Determination of intracellular reactive oxygen species in HepG2

HepG2 cells were grown in 96-well plates and treated as mentioned in section 2.8.4. The intracellular reactive oxygen species (ROS) formation after the induction of lipid accumulation was measured adding DCFDA (25 μmol L^{-1}). After 1 h, the cells were washed with PBS and the fluorescence intensity was detected using a fluorescence microplate reader (Cytation 5, Biotek, Winooski, VT, USA) at 485/ 530 nm excitation/emission wavelength, respectively (Rebollo-Hernanz et al., 2019).

2.8.7. Evaluation of cellular lipid accumulation

For lipid staining with Oil Red O (ORO), HepG2 cells were seeded into 24–well plates and cotreated for 24 h as mentioned in 2.8.4. After that, cells were fixed with formalin and incubated (30 min) with a working solution of ORO, prepared dissolving ORO stock solution (0.35 % w/v Oil Red O in isopropanol overnight) in distilled water (3:2) (Rebollo-Hernanz et al., 2019). To visualize lipid droplets microscopic images were taken, and ORO staining was eluted with pure isopropanol. The absorbance was read at 500 nm by triplicate. After normalization with cell viability, results were expressed as a fold change in lipid accumulation compared to the non-treated cells (control).

2.8.8. Lipolysis assessment

The accumulation of intracellular triacylglycerides (TAG) and lipase activity were performed on the cell lysates (40 μL) from PA-treated HepG2 cells (500 μmol L^{-1}) after the 24 h co-treatment with the CSF or the CSE digested fractions (200 μg mL^{-1}) (section 2.8.4.) with colorimetric assay kits (Spinreact, Barcelona, Spain) according to the manufacturer's instructions (Rebollo-Hernanz et al., 2022). The glycerol was quantified in the culture media (20 μL) collected after the treatment using a glycerol cell-based assay kit (Spinreact, Barcelona, Spain) according to manufacturer's instructions.

2.8.9. Evaluation of intracellular cholesterol and HMGCR inhibitory activity

Intracellular cholesterol (CHO) was determined in the cell lysates (40 μL) (section 2.8.4.) by a colorimetric cholesterol assay kit according to the manufacturer's instructions (Spinreact, Barcelona, Spain). The HMGCR inhibitory activity of cell lysates (20 μL) was analyzed using the commercial HMGCR Assay (Sigma, Madrid, Spain) according to the manufacturer's instructions using a microplate reader.

2.9. Statistical analysis

The results were expressed as the mean ± standard deviation (SD) of at least three independent experiments ($n = 3$). Statistical evaluation was conducted using one-way analysis of variance (ANOVA) followed by the post hoc Tukey test. Significance was attributed to differences with a p-value <0.05. Univariate and bivariate analyses were carried out using SPSS 26.0 software. Principal component analysis (PCA) and hierarchical cluster analysis were employed to categorize the CSF and CSE digestion fractions based on their composition and their hypolipidemic and lipid-lowering properties *in vitro*. Multivariate analysis, including PCA and hierarchical clustering, was performed using XLSTAT2021. Graphical representations were generated using GraphPad Prism 9.0 (GraphPad Software, Inc., San Diego, CA, USA).

3. Results and discussion

3.1. Changes in the CSF and the CSE composition throughout in vitro digestion

The cocoa shell ingredients (CSF and CSE) displayed a different chemical composition, which was affected by the standardized *in vitro* digestion protocol (INFOGEST). The CSF exhibited 13.6 % of proteins, consistent with previously reported values (Okiyama et al., 2017). During the simulated digestion, the CSF proteins remained in the non-digested fraction (13.1–15.4 %), not being detected in the digested fractions. Likewise, the CSE exhibited lower protein content (5.4 %) which decreased to trace amounts in the digested fractions (see Supplementary Table 1). In terms of carbohydrate composition, the raw CSF exhibited 396 μg mg^{-1} of total sugars with galacturonic acid (44 mol %) and glucose (35 mol %) as the major sugars. This profile reflects CSF dietary fiber was mainly constituted by pectic polysaccharides and cellulose, corroborating the cocoa shell dietary fiber composition previously described (Redgwell et al., 2003). Some CSF pectic polysaccharides were solubilized into the CSF digested fractions (135.9–394.1 μg mg^{-1}) comprised mainly of galacturonic acid (50–70 mol %), galactose (9–18 mol %) and arabinose (4–13 mol %). The carbohydrates of the non–digested fractions (355.9–390.9 μg mg^{-1}) exhibited a similar profile as the raw CSF. On the other hand, the CSE polysaccharides (346 μg mg^{-1}) displayed as main sugars galacturonic acid (53 mol %), glucose (14 mol %), and galactose (14 mol %), indicating the presence of pectic polysaccharides as soluble dietary fiber, which degraded throughout the *in vitro* digestion reaching the minimum level in the colonic phase (88 μg mg^{-1}).

Regarding phenolic compounds, the CSE displayed a greater concentration (271.4 mg 100 g^{-1}) than the CSF (43.8 mg 100 g^{-1}). The

phenolic compounds were mainly comprised of gallic acid, followed by catechin and protocatechuic acid. The simulated digestion significantly produced changes on the levels and composition of phenolic compounds, triggering the release of hydroxybenzoic acids and flavan-3-ols, and the degradation of flavanols and flavones (Supplementary Tables 2–3). In both cocoa shell ingredients, theobromine (52.8 and 2605.3 mg 100 g^{-1} in CSF and CSE, respectively) showed higher concentrations than phenolic compounds. The phytochemicals in CSF were more stable than those in CSE due to the interactions of the former with fibers mainly cellulose and pectins. These bindings possibly affect both bioaccessibility and bioavailability and could influence the hypolipidemic properties of these cocoa shell-derived ingredients (Jakobek & Matić, 2019).

3.2. The CSF and CSE bind fat during gastrointestinal digestion

In simulated gastric and intestinal conditions, the CSF showed a maximum fat-binding capacity of 4.5 and 4.6 g oil g^{-1}, respectively, while CSE experimented a higher maximum fat bound (5.5 and 5.6 g oil g^{-1} in gastric and intestinal conditions, respectively) (Fig. 2). This remarkably fat-binding capacity can be attributed to the pectic polysaccharides, which constituted the soluble dietary fiber of these cocoa shell ingredients (Zhang et al., 2015). This ability might be associated with the general hypolipidemic activity of CSF and CSE, as it could increase fecal fat excretion and thus reduce serum lipid levels.

3.3. The digested CSF and CSE fractions showed in vitro hypolipidemic properties

The RMCS capacity is a new intervention target for the treatment of hyperlipidemia and obesity. The results (Fig. 3A) indicate that CSF showed a significant decrease ($p < 0.05$) in RMCS capacity during the digestion process from the oral (61 %) to gastric, intestinal and colonic phases (47–36 %). However, the CSE showed a significant increase ($p < 0.05$) in RMCS ability, from 35 % to 48 % in the intestinal phase, reaching 97 % in the gastric phase. This increase could be due to the changes in the CSE phenolic and polysaccharide composition that took place during the digestion process, especially those related to catechins ($r = 0.792$, $p < 0.05$) and galacturonic acid ($r = 0.955$, $p < 0.01$) (Fig. 4B, Supplementary Table 5). Previous studies have supported the ability of catechins to reduce the solubility of cholesterol micelles by the formation of insoluble cholesterol co-precipitates (Ikeda et al., 2010; Sakakibara et al., 2019). Likewise, pectins, composed by a backbone of

Fig. 2. Fat binding capacity of the cocoa shell flour (CSF) and the cocoa shell extract (CSE) under gastric (GP) and gastrointestinal conditions (IP).

galacturonic acid, have demonstrated, in both animal and humans, to produce viscous solutions that trap cholesterol as well as other essential constituents (bile acids) for micelles formation (Silva et al., 2021). Therefore, these ingredients could reduce the cholesterol solubility by preventing its binding to the mixed micelle, delaying its absorption by the intestinal epithelium and, consequently, its bioavailability.

In addition, the CSF and the CSE oral phases showed capacity to bind primary bile acids (5 and 13 %, respectively) (Fig. 3B), which increased during the digestion process in both matrixes, highlighting the CSE ability in the colonic phase (88 %). The increase of CSF capacity could be mainly due to the release of phenolic compounds ($r = 0.844$, $p < 0.05$) and methylxanthines ($r = 0.855$, $p < 0.05$) (Fig. 4A, Supplementary Table 5). Likewise, the changes in CSE capacity revealed significant correlations with (+)-catechin ($r = 0.876$, $p < 0.05$), (−)-epicatechin ($r = 0.781$, $p < 0.05$) and galacturonic acid ($r = 0.995$, $p < 0.01$) (Fig. 4B, Supplementary Table 5). Previous studies have confirmed that (poly) phenols are able to bind to primary bile acids and thus, prevent their reabsorption from the intestine; and, in turn, reduce the overall bile acid reservoir. As a result, more cholesterol is converted into bile acids to maintain a constant level (Ngamukote et al., 2011). Furthermore, the galacturonic acid polysaccharides have demonstrated the ability to bind primary bile acids due to their viscosity and the hydrophobic or hydrophilic interactions in the gel matrix (Dongowski, 2007; Gunness et al., 2021; Naumann et al., 2020). Therefore, these results indicate the cocoa shell ingredients may bind primary bile acids in the intestine, reducing their reabsorption and triggering their *de novo* synthesis from circulating cholesterol.

Secondary bile acids, produced during bacterial metabolism in the colon, have been the subject of interest in recent years due to their important role in colorectal cancer (Collins et al., 2023). The CSF capacity to bind secondary bile acids (Fig. 3C) is similar in oral and colonic phases (42 %), however the CSE capacity decreased significantly ($p < 0.05$) in the colonic phase (33 %). This ability appears to be significantly related to the phenolic compounds, in the case of CSF with the N-Caffeoyl-L-DOPA *cis* ($r = 0.829$, $p < 0.05$), and in CSE with protocatechuic acid ($r = 0.902$, $p < 0.01$), N-coumaroyl-L-tyrosine ($r = 0.998$, $p < 0.01$) and N-caffeoyl-L-DOPA *cis* ($r = 0.985$, $p < 0.01$) (Fig. 4, Supplementary Table 5). In this regard, protocatechuic acid has demonstrated the ability to significantly reduce the level of secondary bile acids and modify the intestinal microbiota favoring a healthier population and reducing the risk of colon cancer (Gao et al., 2022; Zhao et al., 2021).

The inhibition of gastric and pancreatic lipase has become a key in the prevention of dyslipidemia. The digested gastric and intestinal fractions of CSF demonstrated high ability to inhibit the lipase activity (106 and 51 %, respectively, $p < 0.01$) (Fig. 3D). Likewise, CSE displayed this ability in all digested fractions (41–80 %). Then, the phenolic compounds released and their changes throughout the *in vitro* digestion could be associated with the improvement of lipase inhibition ability, as previously reported by Buchholz & Melzig (2015). Accordingly, the CSF results presented a robust significant correlation with protocatechuic acid ($r = 0.967$, $p < 0.01$) and catechin ($r = 0.998$, $p < 0.01$) (Fig. 4A, Supplementary Table 5). Similarly, the CSE ability depicted strong statistically significant correlations with catechin (0.983, $p < 0.01$) and N-caffeoyl-L-DOPA *cis* ($r = 0.847$, $p < 0.05$) (Fig. 4B, Supplementary Table 5). *In vitro* and *in vivo* studies have exhibited the ability of flavonoids such as catechin and protocatechuic acid as well as other hydroxycinnamic acids to inhibit lipase activity (Martinez-Gonzalez et al., 2017; Nagao et al., 2005). Phenolic compounds could interact with lipase through hydrophobic interactions, hydrogen bonds, and π-π interactions of the aromatic rings which produce changes in the lipase structure, modifying its activity (Martinez-Gonzalez et al., 2017). Furthermore, the lipase activity inhibition showed a robust correlation with the CSE ability to RMCS ($r = 0.993$, $p < 0.01$) and with the CSF and CSE digested fraction's ability to bind primary bile acids ($r = 0.886$; $p < 0.05$ and $r = 0.968$, $p < 0.01$, respectively) (Supplementary Tables 5,6). Hence, the results corroborate that the bile acids attachment reduce the
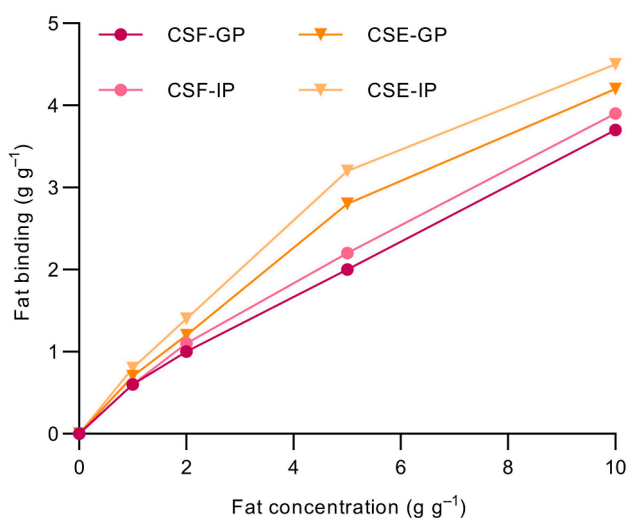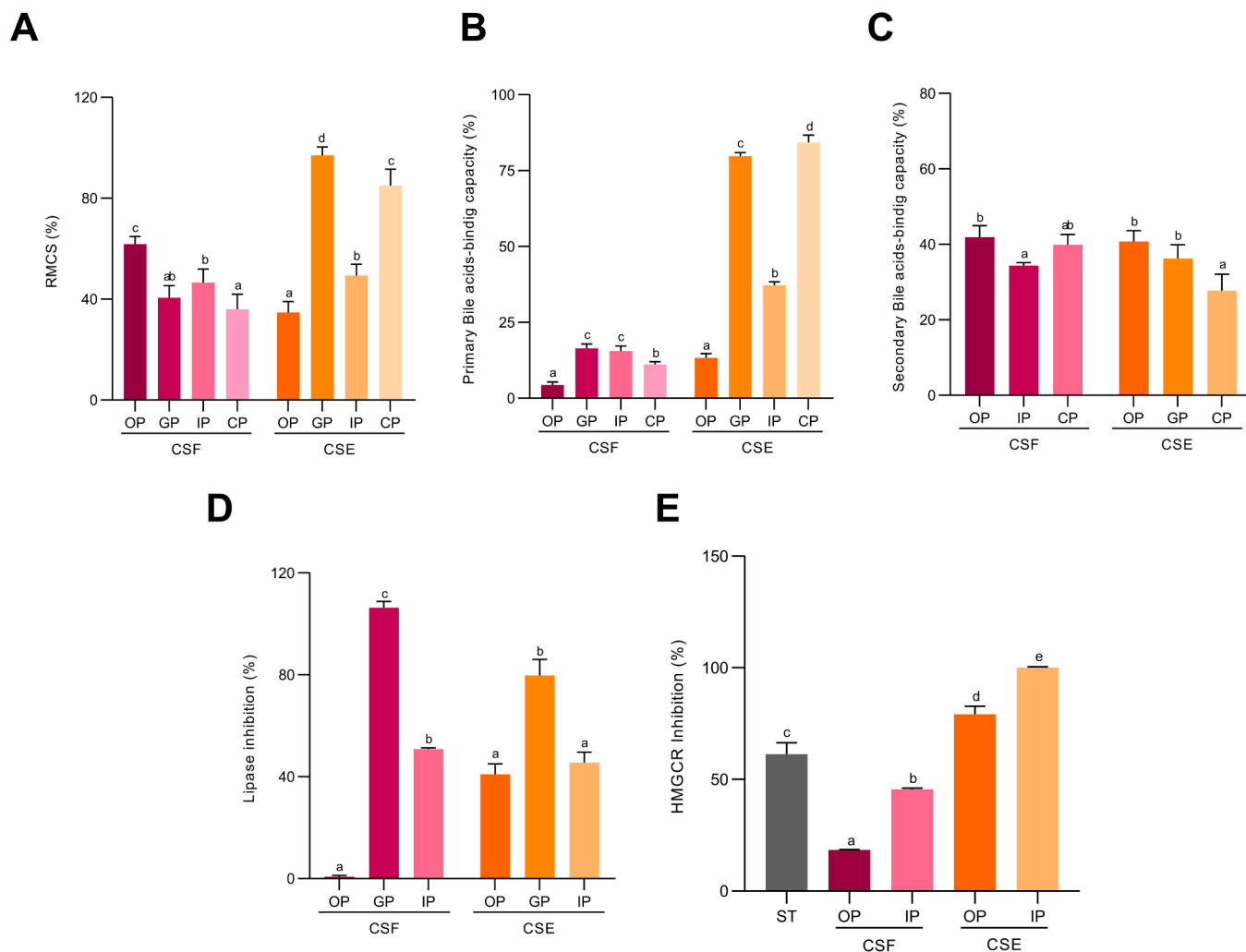
Fig. 3. *In vitro* capacity to reduce micellar cholesterol solubility (RMCS) (A), primary (B) and secondary (C) bile-acids binding ability; lipase (D) and hydroxymethylglutaryl-Co-enzyme A reductase (HMGCR) inhibition (E) capacities of oral (OP), gastric (GP), intestinal (IP) and colonic (CP) digested fractions of the cocoa shell flour (CPF) and the cocoa shell extract (CPE). Bars with different letters denote significant differences between the digested fractions of the CSF or the CSE according to ANOVA and Tukey's multiple range test ($p < 0.05$).

emulsification capacity and the pancreatic lipase activity, preventing fatty acids liberation and their absorption.

In addressing lipid accumulation, the inhibition of HMGCR assumes a critical role in the hypercholesterolemia management (Gesto et al., 2020). In this regard, the oral and intestinal digested fractions of CSF were able to reduce HMGCR activity (18 % and 46 %, respectively) (Fig. 3E). Regarding CSE, the intestinal fraction exhibited the total inhibition of this enzyme, whereas the oral fraction showed lower capacity (79 %). These findings suggest a potential interaction of the CSF and CSE phenolic compounds with the active binding site of HMGCR (Gesto et al., 2020). Thus, these cocoa shell ingredients hold the potential to inhibit HMGCR in organs such as the liver, resulting in a reduction of cholesterol synthesis.

3.4. The non-digested fractions further enhanced the CSF in vitro hypolipidemic properties

The gastric non-digested fraction of CSF demonstrated a significant reduction ($p < 0.05$) in its cholesterol-binding ability at pH 2 (38 %) compared to the original material (69 %). Similarly, a notable decrease ($p < 0.05$) from 56 % to 34 % was observed in the intestinal phase at pH 7 (Fig. 5A). Conversely, the non-digested fractions of CSF exhibited significantly higher capacity to bind bile salts (67–91 %) than the raw

flour (62 %), standing out the gastric and colonic phases (Fig. 5B). In addition, the ability to inhibit the lipase activity varied with the presence (23–52 % BBSS+) or absence (58–99 % BBSS-) of bile salts (BBSS), being this capacity significantly higher ($p < 0.05$) in the intestinal phase (Fig. 5C). The results obtained from the non-digested fractions indicate that *in vitro* gastrointestinal digestion maintain or improve the CSF ability to inhibit pancreatic lipase as well as to bind cholesterol and bile salts. These capacities might be associated with the direct inhibitory effects of phenolic compounds and the noteworthy dietary fiber content in CSF (39–66 %). As known dietary fiber can effectively bind organic substances like cholesterol and inhibit the emulsifying activity and reabsorption of bile salts (Capuano, 2017; Di Gregorio et al., 2021; Hong et al., 2012). Additionally, the dietary fiber could potentially bind to lipids, create a protective coating around lipid droplets or trap lipase limiting their accessibility (Taladrid et al., 2023). Changes in these properties may be related to pH variations associated with digestion, which cause transformations in glycoside bonds and ester linkages, thereby influencing the dietary fiber composition (Yang et al., 2018). Therefore, the non-digested fractions further enhanced the CSF *in vitro* hypolipidemic properties highlighting the potential of this ingredient to decrease lipid absorption during the digestion process.

A

B
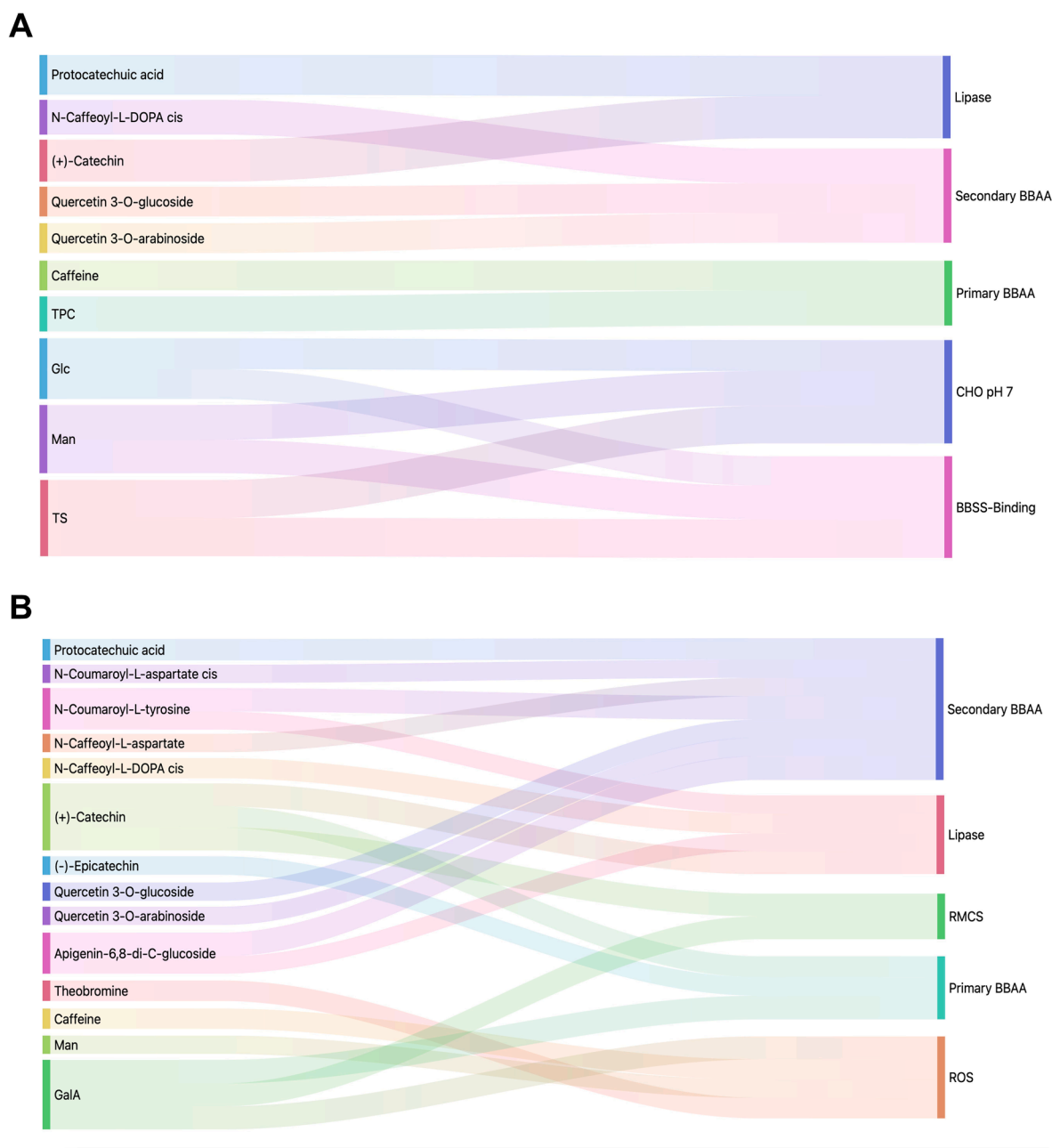
Fig. 4. Sankey diagram depicting the significant ($p < 0.05$) Pearson correlations among the digestion parameters for the cocoa shell flour (CSF), dietary fiber and phenolic's composition, and *in vitro* physiological properties (A). Chord diagram illustrating the significant ($p < 0.05$) Pearson correlations among the digestion parameters for the cocoa shell extract (CSE), dietary fiber and phenolic's composition, and *in vitro* physiological properties (B).

3.5. CSF and CSE lipid-lowering effects in HepG2 cells after digestion

The assessment of the CSF and CSE digested fractions to prevent lipid accumulation was evaluated in a HepG2 cell model after PA stimulation (Fig. 6A). Intracellular lipid accumulation (steatosis), one of the main characteristics of NAFLD, caused by an imbalance between *de novo* lipogenesis, lipid degradation and increased uptake of circulating free fatty acids, was qualitatively assessed by ORO staining (Rafiei et al., 2023). Co-treatment with the CSF and CSE oral and intestinal digested fractions decreased the lipid content regarding PA-treated cells (Fig. 6B). Other NAFLD feature is the oxidative stress associated to cell damage. PA exposure of hepatocytes produced an increase in reactive oxygen species (ROS) production (1.4-fold, $p < 0.05$) (Fig. 6C), probably due to the higher NAPDH oxidase activity or by mitochondria dysfunction (Delli Bovi et al., 2021; Rebollo-Hernanz et al., 2022). This

ROS increase was mitigated when cells were co-treated with CSF or CSE digested fractions, mainly with the intestinal (40 % and 97 %, respectively, $p < 0.05$). The CSF effect was strongly correlated with flavonols ($r = 0.967, p < 0.01$), while in CSE was associated with methylxanthines ($r = 0.854, p < 0.05$) and total phenolic compounds ($r = 0.849, p < 0.05$) (Supplementary Tables 4 and 5). The lipid-lowering attributes appear to be closely linked to the phytochemicals of cocoa shell ingredients, which display a remarkable ability to decrease oxidative stress that is maintained during gastrointestinal digestion (Cañas et al., 2023; Rebollo-Hernanz et al., 2022).

Increased lipid accumulation (30 %, $p < 0.05$) was observed in PA-treated hepatocytes (Fig. 6D) because of the PA ability to decrease the AMP-activated protein kinase (AMPK) activity (Asrih et al., 2015). The increase of intracellular lipids was reduced when cells were cotreated with CSF digested fractions, being significant in case of intestinal
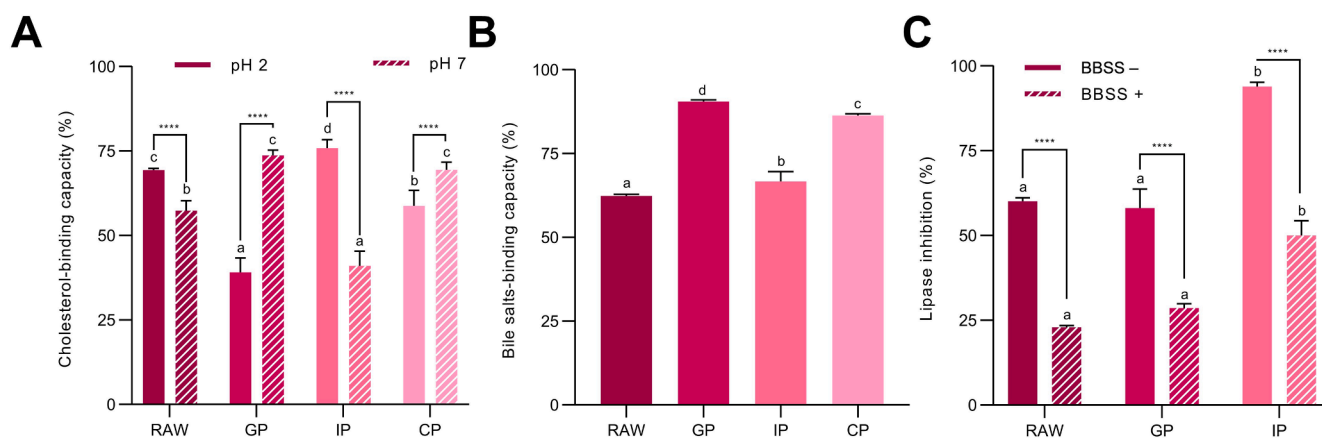
Fig. 5. *In vitro* cholesterol binding capacity (A), bile salts binding capacity (B) and lipase inhibition (C) in presence or absence of bile salts (BBSS +/-) of raw, gastric (GP), intestinal (IP) and colonic (CP) non-digested fractions of the cocoa shell flour (CSF). Bars with different letters denote significant differences between the non-digested fractions of the CSF according to ANOVA and Tukey's multiple range test ($p < 0.05$).

fraction (78 %, $p < 0.05$) and, in CSE oral and intestinal digested fractions (82 and 122 %, $p < 0.05$, respectively), even reaching the basal lipid levels with the CSE intestinal fraction (Fig. 6D). A similar response was observed for the intracellular TAG content (Fig. 6E). All co-treatments significantly reduced (60–90 %, $p < 0.05$) the TAG increase caused by PA, generally achieving similar TAG levels to non-treated cells (36.5 mmol mg^{-1}). This intracellular TAG accumulation is regulated by lipolysis, and PA stimulation significantly reduced (40 %, $p < 0.05$) lipase activity compared to the non-treated cells (Fig. 6F). Only the CSF oral and the CSE intestinal digested fractions were able to significantly reverse the decrease of the enzymatic activity (28 and 78 %, $p < 0.05$, respectively). Interestingly, all co-treatments reverted the reduction in glycerol release produced by PA (35 %), exhibiting a significant glycerol increase (27–80 %, $p < 0.05$) (Fig. 6G).

The PA hepatocytes stimulation resulted in an increase of the intracellular cholesterol from 54.8 mmol mg^{-1} in non-treated cells to 78.4 mmol mg^{-1} in PA-exposed cells, being significantly reduced by all co-treatments reaching the levels of the non-treated cells except for CSE intestinal phase (Fig. 6H). Similarly, we assessed HMGCR activity in cellular lysates to disclose the mechanism responsible for the cholesterol reduction (Fig. 6I). The cells treated with PA demonstrated elevated HMGCR activity (14 %, $p < 0.05$) compared to the non-treated cells. Notably, the cells co-treated with the CSF and CSE digested fractions exhibited a substantial decrease in HMGCR activity, regarding both the PA-stimulated and the non-treated cells with a residual activity close to 60 % for CSF and 70 % for CSE. HMGCR is the rate-limiting enzyme in the cholesterol biosynthetic pathway (Jiang et al., 2018; Mahdavi et al., 2020). The HMGCR inhibition by the cocoa shell treatments is consistent with the observed reduction in intracellular cholesterol concentration, whereby CSF and CSE are able to significantly reduce the synthesis and storage of intracellular hepatic cholesterol.

Hierarchical cluster analysis (Fig. 6J) depicted the grouping of samples based on their effectiveness in modulating lipid metabolism in HepG2 cells following palmitic acid (PA) stimulation. The results indicated the formation of two clusters: the first comprised PA-treated cells, while the second encompassed non-treated cells along with cells co-treated with PA and both the digested fractions of CSF and CSE. Within this second cluster, non-treated cells and those treated with digested intestinal fraction of CSE were grouped together, indicating that the CSE digested intestinal fraction exhibited the highest efficacy in regulating lipid metabolism and mitigating the adverse effects induced by PA. Consequently, since the lipid-lowering properties of CSF and CSE were maintained after simulated digestion, these food ingredients may serve as regulators of hepatic lipid accumulation pathways, being useful in preventing hepatic lipid accumulation and, ultimately, NAFLD.

3.6. The hypolipidemic properties of CSF and CSE are influenced by the composition, digestion and matrix

Multivariate analyses (PCA and hierarchical cluster analysis) were performed to further investigate the relationship between CSF and CSE composition and their hypolipidemic properties through gastrointestinal digestion (Fig. 7A–C). Seven different principal components (PCs) were obtained. Fig. 7A depicts the PC loadings for the first two PCs. We can observe that PC1 explained 44.7 % of the whole variability and integrated variables such as methylxanthine (10 %), TPC (9.9 %) or galacturonic acid (9.6 %) contents. On the other hand, PC2 (18.9 % of the variability) was influenced by mannose and glucose composition (16.9 and 13.7 % respectively), RMCS capacity (9.9 %) and primary bile salts binding ability (9.8 %). The PC scores (Fig. 7B) and the hierarchical cluster analysis (Fig. 7C) categorized the samples into two groups. In cluster 1 we find CSF and its different digestion phases with a higher contribution of sugar composition to their hypolipidemic properties. In cluster 2 we find CSE and its different digestion phases with a higher contribution of phenolic compounds to their overall hypolipidemic activity. This classification into 2 groups may be due to the differences between the two matrices and how these affect their properties during the digestion process. In the case of CSF, being a flour, this dietary fiber-rich matrix protects phenolic compounds, which have been shown to be linked to hypolipidemic properties, by releasing them slowly and preventing their degradation and/or conversion into other compounds. On the other hand, in the case of CSE, the phenolic compounds are much more exposed both to carry out their hypolipidemic activity and suffer degradations that take place during the digestion process. Consequently, either gastrointestinal digestion or the matrix affects to the composition and hypolipidemic properties of CSF and CSE.

Fig. 7D summarizes the hypolipidemic mechanisms of CSF and CSE at the intestinal level as well as their lipid-lowering properties at the hepatic level. In the intestine, these cocoa shell ingredients would be able to inhibit lipase activity, preventing the fatty acids release that can cross the intestinal epithelium and transform back into triglycerides in the bloodstream. Additionally, they could destabilize cholesterol micelles and bind to free cholesterol, thereby decreasing its absorption. Likewise, they may bind to free bile salts or acids, diminishing their reabsorption and their conversion to cholesterol in the liver. At the hepatic level, these ingredients would be able to reverse the effect caused by PA, reducing oxidative stress and intracellular lipid accumulation. This is accompanied by an increase in lipase activity, leading to a decrease in intracellular TAGs, and a reduction in HMGCR activity along with a corresponding diminution of intracellular cholesterol. These events of the metabolic cascade could be induced by the ability of the CSF and CSE phytochemicals to inhibit the blockade produced by PA
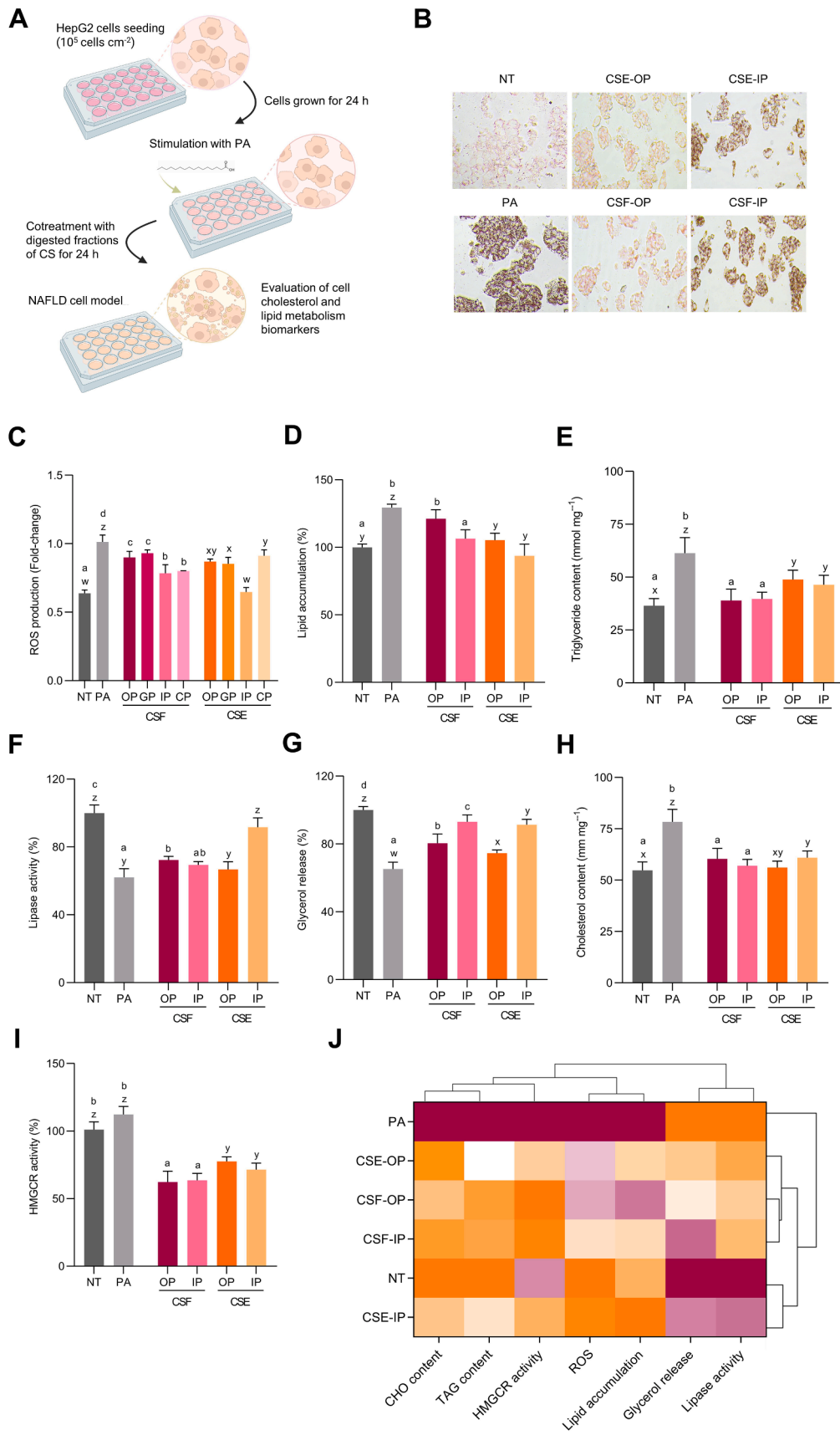
(caption on next page)

Fig. 6. Illustrative diagram depicting HepG2 cells stimulation with palmitic acid (PA) and co-treatment with the digested fractions of cocoa shell flour (CSF) and the cocoa shell extract (CSE) (A) qualitative (Oil Red O) lipid accumulation (B); Reactive oxygen species (ROS) production (C) quantitative lipid accumulation (D); triglyceride content (E); lipase activity (F); glycerol release (G); cholesterol content (H); hydroxymethylglutaryl-Co-enzyme A reductase (HMGCR) activity (I) in HepG2 cells: non treated (NT), treated with PA and co-treated with PA and oral (OP), gastric (GP), intestinal (IP) and colonic (CP) digested fractions of CSF and CSE. Hierarchical cluster analysis (J). Bars with different letters denote significant differences between the digested phases of the CSF or the CSE according to ANOVA and Tukey's multiple range test ($p < 0.05$). (For interpretation of the references to color in this figure legend, the reader is referred to the web version of this article.)
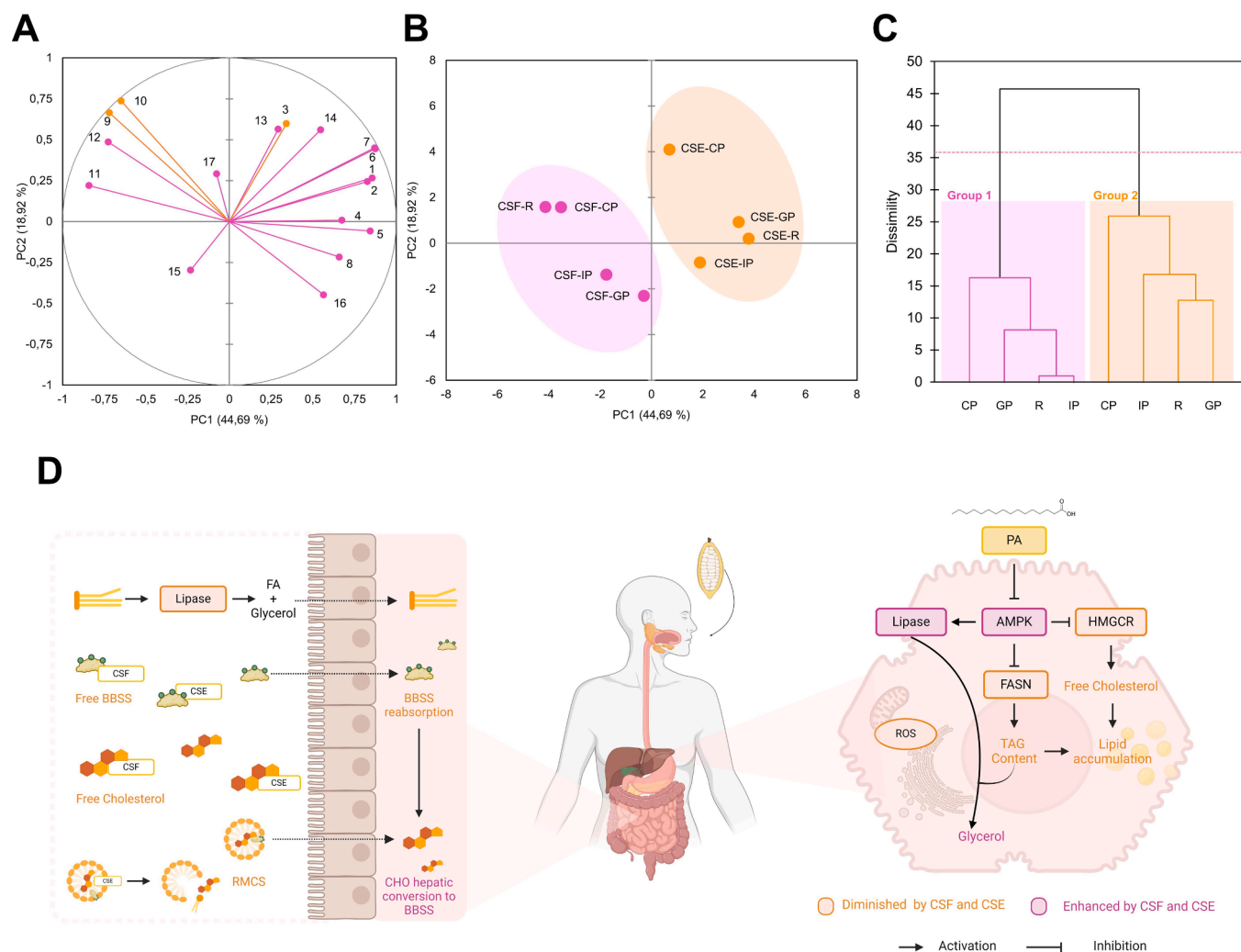
Fig. 7. Principal component (PC) analysis (loadings in (A) and PC scores in (B)). Dendrogram of the hierarchical cluster analysis classifying samples (C). Illustrative diagram summarizing the main hypolipidemic effects in the digestive system and the main signaling pathways modulated by the CSF and CSE digested fractions on the hepatic lipid metabolism (D). Number identification: 1: Hydroxibenzoic acids. 2: N-Phenylpropenoyl-L-amino acids. 3: Flavan-3-ols. 4: Flavonols. 5: Flavones. 6: Methylxantines. 7: Total phenolic content. 8: Total protein content. 9: Glucose. 10: Mannose. 11: Galacturonic acid. 12: Total sugar content. 13. Reduction of micellar cholesterol solubility capacity. 14: Primary bile salts binding. 15: Secondary Bile Salts binding. 16: Lipase inhibition. 17: Reactive oxygen Species scavenging in HepG2 cells. R—Raw; GP—gastric phase; IP—intestinal phase; CP—colonic phase.

on AMPK and the fatty acid synthase (FASN), as previously reported (Singh et al., 2020; Xu et al., 2023).

4. Conclusion

This study represents a pioneering exploration into the effects of simulated digestion on the hypolipidemic potential of cocoa shell ingredients (CSF and CSE). Noteworthy findings reveal that the CSF and CSE digested fractions exhibited the enhanced *in vitro* capacities to reduce micellar cholesterol solubility, bind primary and secondary bile acids, and inhibit the lipase and HMGCR activities, preventing the cholesterol and fats absorption. The CSF non-digested fractions exhibited considerable *in vitro* hypolipidemic properties, thereby reinforcing

the consistence of this ingredient in attenuating lipid absorption. Furthermore, the CSF and CSE digested fractions diminished lipid accumulation in HepG2 cell model. Both CSF and CSE effectively mitigated palmitic acid-induced accumulation of intracellular lipids, triacylglycerides, and cholesterol, by stimulating lipolysis and inhibiting HMGCR activity. Phenolic compounds and dietary fiber are significantly associated to the observed hypolipidemic effects of cocoa shell ingredients. Hence, this study advances the understanding of the effect of simulated digestion on the intestinal and hepatic lipid-lowering properties of cocoa shell ingredients. Due to their demonstrated *in vitro* efficacy in reducing lipid absorption and reversing its hepatic accumulation, CSF and CSE emerge as promising food ingredients for the prevention of diseases related to the lipid accumulation, and promoting

overall health. Nevertheless, to conclude this research, future dietary intervention studies are required to confirm these promising findings *in vivo*.

CRediT authorship contribution statement

Cheyenne Braojos: Writing – original draft, Visualization, Software, Methodology, Investigation, Formal analysis, Data curation, Conceptualization. **Miguel Rebollo-Hernanz:** Writing – review & editing, Methodology, Formal analysis, Conceptualization. **Silvia Cañas:** Writing – review & editing, Methodology. **Yolanda Aguilera:** Writing – review & editing, Visualization, Methodology. **Alicia Gil-Ramírez:** Writing – review & editing, Visualization, Methodology. **Vanesa Benítez:** Writing – review & editing, Writing – original draft, Visualization, Validation, Supervision, Resources, Methodology, Funding acquisition, Conceptualization. **Maria A. Martín-Cabrejas:** Writing – review & editing, Writing – original draft, Supervision, Resources, Project administration, Methodology, Funding acquisition, Conceptualization.

Declaration of competing interest

The authors declare that they have no known competing financial interests or personal relationships that could have appeared to influence the work reported in this paper.

Data availability

Data will be made available on request.

Acknowledgements

Appendix A. Supplementary data

Supplementary data to this article can be found online at https://doi.org/10.1016/j.foodres.2024.115037.

References

Asrih, M., Montessuit, C., Philippe, J., & Jornayvaz, F. R. (2015). Free fatty acids impair FGF21 action in HepG2 cells. *Cellular Physiology and Biochemistry, 37*(5), 1767–1778. https://doi.org/10.1159/000438540

Benítez, V., Rebollo-Hernanz, M., Aguilera, Y., Bejerano, S., Cañas, S., & Martín-Cabrejas, M. A. (2021). Extruded coffee parchment shows enhanced antioxidant, hypoglycaemic, and hypolipidemic properties by releasing phenolic compounds from the fibre matrix. *Food and Function, 12*(3), 1097–1110. https://doi.org/10.1039/d0fo02295k

Benítez, V., Rebollo-Hernanz, M., Braojos, C., Cañas, S., Gil-Ramírez, A., Aguilera, Y., & Martín-Cabrejas, M. A. (2023). Changes in the cocoa shell dietary fiber and phenolic compounds after extrusion determine its functional and physiological properties. *Current Research in Food Science, 6*, Article 100516. https://doi.org/10.1016/j.crfs.2023.100516

Brodkorb, A., Egger, L., Alminger, M., Alvito, P., Assunção, R., Ballance, S., Bohn, T., Bourlieu-Lacanal, C., Boutrou, R., Carrière, F., Clemente, A., Corredig, M., Dupont, D., Dufour, C., Edwards, C., Golding, M., Karakaya, S., Kirkhus, B., Le Feunteun, S., & Recio, I. (2019). INFOGEST static *in vitro* simulation of gastrointestinal food digestion. *Nature Protocols, 14*(4), 991–1014. https://doi.org/10.1038/s41596-018-0119-1

Buchholz, T., & Melzig, M. F. (2015). Polyphenolic compounds as pancreatic lipase inhibitors. *Planta Medica, 81*, 771–783. https://doi.org/10.1055/s-0035-1546173

Cañas, S., Rebollo-Hernanz, M., Bermúdez-Gómez, P., Rodríguez-Rodríguez, P., Braojos, C., Gil-Ramírez, A., Benítez, V., Aguilera, Y., & Martín-Cabrejas, M. A. (2023). Radical scavenging and cellular antioxidant activity of the cocoa shell phenolic compounds after simulated digestion. *Antioxidants, 12*(5). https://doi.org/10.3390/antiox12051007

Cañas, S., Rebollo-Hernanz, M., Braojos, C., Benítez, V., Ferreras-Charro, R., Dueñas, M., Aguilera, Y., & Martín-Cabrejas, M. A. (2022). Gastrointestinal fate of phenolic compounds and amino derivatives from the cocoa shell: An *in vitro* and *in silico* approach. *Food Research International, 162*, Article 112117. https://doi.org/10.1016/j.foodres.2022.112117

Cantele, C., Rojo-Poveda, O., Bertolino, M., Ghirardello, D., Cardenia, V., Barbosa-Pereira, L., & Zeppa, G. (2020). *In vitro* bioaccessibility and functional properties of phenolic compounds from enriched beverages based on cocoa bean shell. *Foods, 9* (6). https://doi.org/10.3390/FOODS9060715

Capuano, E. (2017). The behavior of dietary fiber in the gastrointestinal tract determines its physiological effect. *Critical Reviews in Food Science and Nutrition, 57*(16), 3543–3564. https://doi.org/10.1080/10408398.2016.1180501

Cinar, Z.Ö., Atanassova, M., Tumer, T. B., Caruso, G., Antika, G., Sharma, S., Sharifi-Rad, J., & Pezzani, R. (2021). Cocoa and cocoa bean shells role in human health: An updated review. *Journal of Food Composition and Analysis, 103*, Article 104115. https://doi.org/10.1016/j.jfca.2021.104115

Collins, S. L., Stine, J. G., Bisanz, J. E., Okafor, C. D., & Patterson, A. D. (2023). Bile acids and the gut microbiota: Metabolic interactions and impacts on disease. *Nature Reviews Microbiology, 21*(4), 236–247. https://doi.org/10.1038/s41579-022-00805-x

Delli Bovi, A. P., Marciano, F., Mandato, C., Siano, M. A., Savoia, M., & Vajro, P. (2021). Oxidative stress in non-alcoholic fatty liver disease. An updated mini review. *Frontiers in Medicine, 8*, Article 595371. https://doi.org/10.3389/fmed.2021.595371

Di Gregorio, M. C., Cautela, J., & Galantini, L. (2021). Physiology and PHYSICAL CHEMISTRY OF BILE ACIDs. *International Journal of Molecular Sciences, 22*(4), 1–23. https://doi.org/10.3390/IJMS22041780

Dongowski, G. (2007). Interactions between dietary fibre-rich preparations and glycoconjugated bile acids *in vitro*. *Food Chemistry, 104*(1), 390–397. https://doi.org/10.1016/j.foodchem.2006.11.053

Fernandes, P. A. R., Ferreira, S. S., Bastos, R., Ferreira, I., Cruz, M. T., Pinto, A., Coelho, E., Passos, C. P., Coimbra, M. A., Cardoso, S. M., & Wessel, D. F. (2019). Apple pomace extract as a sustainable food ingredient. *Antioxidants, 8*(6), Article 189. https://doi.org/10.3390/antiox8060189

Gao, Y., Tian, R., Liu, H., Xue, H., Zhang, R., Han, S., Ji, L., Huang, W., Zhan, J., & You, Y. (2022). Research progress on intervention effect and mechanism of protocatechuic acid on nonalcoholic fatty liver disease. *Critical Reviews in Food Science and Nutrition, 62*(32), 9053–9075. https://doi.org/10.1080/10408398.2021.1939265

Gesto, D. S., Pereira, C. M. S., Cerqueira, N. M. F. S., & Sousa, S. F. (2020). An atomic-level perspective of HMG-CoA-reductase: The target enzyme to treat hypercholesterolemia. *Molecules, 25*(17), 3891. https://doi.org/10.3390/molecules25173891

Gunness, P., Zhai, H., Williams, B. A., Zhang, D., & Gidley, M. J. (2021). Pectin and mango pulp both reduce plasma cholesterol in pigs but have different effects on triglycerides and bile acids. *Food Hydrocolloids, 112*. https://doi.org/10.1016/j.foodhyd.2020.106369

Herrera, T., Aguilera, Y., Rebollo-Hernanz, M., Bravo, E., Benítez, V., Martínez-Sáez, N., Arribas, S. M. S. M., del Castillo, M. D. M. D., & Martín-Cabrejas, M. A. M. A. (2018). Teas and herbal infusions as sources of melatonin and other bioactive non-nutrient components. *LWT - Food Science and Technology, 89*, 65–73. https://doi.org/10.1016/j.lwt.2017.10.031

Hong, Y., Zi-jun, W., Jian, X., Ying-jie, D., & Fang, M. (2012). Development of the dietary fiber functional food and studies on its toxicological and physiologic properties. *Food and Chemical Toxicology, 50*(9), 3367–3374. https://doi.org/10.1016/j.fct.2012.05.011

Ikeda, I., Yamahira, T., Kato, M., & Ishikawa, A. (2010). Black-tea polyphenols decrease micellar solubility of cholesterol *in vitro* and intestinal absorption of cholesterol in rats. *Journal of Agricultural and Food Chemistry, 58*(15), 8591–8595. https://doi.org/10.1021/jf1015285

Jakobek, L., & Matić, P. (2019). Non-covalent dietary fiber - Polyphenol interactions and their influence on polyphenol bioaccessibility. *Trends in Food Science and Technology, 83*, 235–247. https://doi.org/10.1016/j.tifs.2018.11.024

Jiang, S. Y., Li, H., Tang, J. J., Wang, J., Luo, J., Liu, B., Wang, J. K., Shi, X. J., Cui, H. W., Tang, J., Yang, F., Qi, W., Qiu, W. W., & Song, B. L. (2018). Discovery of a potent HMG-CoA reductase degrader that eliminates statin-induced reductase accumulation and lowers cholesterol. *Nature Communications, 9*(1). https://doi.org/10.1038/s41467-018-07590-3

Levin, S. J., Johnston, C. G., & Boyle, A. J. (1961). Spectrophotometric determination of several bile acids as conjugates: Extraction with ethyl acetate. *Analytical Chemistry, 33*(10), 1407–1411. https://doi.org/10.1021/AC60178A041/ASSET/AC60178A041.FP.PNG_V03

Li, X., Chen, Y., Li, S., Chen, M., Xiao, J., Xie, B., & Sun, Z. (2019). Oligomer procyanidins from lotus seedpod regulate lipid homeostasis partially by modifying fat emulsification and digestion. *Journal of Agricultural and Food Chemistry, 67*(16), 4524–4534. https://doi.org/10.1021/ACS.JAFC.9B01469/SUPPL_FILE/JF9B01469_SI_001.PDF

Mahdavi, A., Bagheriya, M., Fakheran, O., Reiner, Ž., Xu, S., & Sahebkar, A. (2020). Medicinal plants and bioactive natural compounds as inhibitors of HMG-CoA reductase: A literature review. *BioFactors, 46*, 906–926. https://doi.org/10.1002/biof.1684

Mariati, F., Gunjević, V., Boffa, L., & Cravotto, G. (2021). Process intensification technologies for the recovery of valuable compounds from cocoa by-products. *Innovative Food Science and Emerging Technologies, 68*. https://doi.org/10.1016/j.ifset.2021.102601

Martinez-Gonzalez, A. I., Alvarez-Parrilla, E., Díaz-Sánchez, Á. G., De La Rosa, L. A., Núñez-Gastélum, J. A., Vazquez-Flores, A. A., & Gonzalez-Aguilar, G. A. (2017).

Inhibition of lipase by polyphenols. *Food Technology and Biotechnology, 55*(4), 519–530. https://doi.org/10.17113/ftb.55.04.17.5138

Nagao, T., Komine, Y., Soga, S., Meguro, S., Hase, T., Tanaka, Y., & Tokimitsu, I. (2005). Ingestion of a tea rich in catechins leads to a reduction in body fat and malondialdehyde-modified LDL in men 1–3. *The American Journal of Clinical Nutrition, 81*, 122–129. https://doi.org/10.1093/ajcn/81.1.122

Naumann, S., Haller, D., Eisner, P., & Schweiggert-Weisz, U. (2020). Mechanisms of interactions between bile acids and plant compounds—A review. *International Journal of Molecular Sciences, 21*, 1–20. https://doi.org/10.3390/ijms21186495

Ngamukote, S., Mäkynen, K., Thilawech, T., & Adisakwattana, S. (2011). Cholesterol-lowering activity of the major polyphenols in grape seed. *Molecules, 16*(6), 5054–5061. https://doi.org/10.3390/molecules16065054

Nogueira Soares Souza, F., Rocha Vieira, S., Leopoldina Lamounier Campidelli, M., Abadia Reis Rocha, R., Milani Avelar Rodrigues, L., Henrique Santos, P., de Deus Souza Carneiro, J., I., Maria de Carvalho Tavares, & Patrícia de Oliveira, C. (2022). Impact of using cocoa bean shell powder as a substitute for wheat flour on some of chocolate cake properties. *Food Chemistry, 381*. https://doi.org/10.1016/j.foodchem.2022.132215

Noori, M., Jafari, B., & Hekmatdoost, A. (2017). Pomegranate juice prevents development of non-alcoholic fatty liver disease in rats by attenuating oxidative stress and inflammation. *Journal of the Science of Food and Agriculture, 97*, 2327–2332. https://doi.org/10.1002/jsfa.8042

Okiyama, D. C. G., Navarro, S. L. B., & Rodrigues, C. E. C. (2017). Cocoa shell and its compounds: Applications in the food industry. *Trends in Food Science and Technology, 63*, 103–112. https://doi.org/10.1016/j.tifs.2017.03.007

Ontawong, A., Duangjai, A., Muanprasat, C., Pasachan, T., Pongchaidecha, A., Amornlerdpison, D., & Srimaroeng, C. (2019). Lipid-lowering effects of *Coffea arabica* pulp aqueous extract in Caco-2 cells and hypercholesterolemic rats. *Phytomedicine, 52*, 187–197. https://doi.org/10.1016/j.phymed.2018.06.021

Panak Balentić, J., Ačkar, Đ., Jokić, S., Jozinović, A., Babić, J., Miličević, B., Šubarić, D., & Pavlović, N. (2018). Cocoa shell: A by-product with great potential for wide application. *Molecules, 23*(6). https://doi.org/10.3390/molecules23061404

Papillo, V. A., Vitaglione, P., Graziani, G., Gokmen, V., & Fogliano, V. (2014). Release of antioxidant capacity from five plant foods during a multistep enzymatic digestion protocol. *Journal of Agricultural and Food Chemistry, 62*(18), 4119–4126. https://doi.org/10.1021/jf500695a

Rafiei, H., Yeung, M., Kowalski, S., Krystal, G., Elisia, I., Zhu, R., & Juanola, O. (2023). Development of a novel human triculture model of non-alcoholic fatty liver disease and identification of berberine as ameliorating steatosis, oxidative stress and fibrosis. *Frontiers in Pharmacology, 14*, Article 1234300. https://doi.org/10.3389/fphar.2023.1234300

Rebollo-Hernanz, M., Aguilera, Y., Martin-Cabrejas, M. A., & Gonzalez de Mejia, E. (2022). Phytochemicals from the cocoa shell modulate mitochondrial function, lipid and glucose metabolism in hepatocytes via activation of FGF21/ERK, AKT, and mTOR pathways. *Antioxidants, 11*(1). https://doi.org/10.3390/antiox11010136

Rebollo-Hernanz, M., Zhang, Q., Aguilera, Y., Martín-Cabrejas, M. A., & Gonzalez de Mejia, E. (2019). Phenolic compounds from coffee by-products modulate adipogenesis-related inflammation, mitochondrial dysfunction, and insulin resistance in adipocytes, via insulin/PI3K/AKT signaling pathways. *Food and Chemical Toxicology, 132*, Article 110672. https://doi.org/10.1016/j.fct.2019.110672

Redgwell, R., Trovato, V., Merinat, S., Curti, D., Hediger, S., & Manez, A. (2003). Dietary fibre in cocoa shell: Characterisation of component polysaccharides. *Food Chemistry, 81*(1), 103–112. https://doi.org/10.1016/S0308-8146(02)00385-0

Rojo-Poveda, O., Barbosa-Pereira, L., Zeppa, G., & Stévigny, C. (2020). Cocoa bean shell—A by-product with nutritional properties and biofunctional potential. *Nutrients, 12*(4), 1–29. https://doi.org/10.3390/nu12041123

Ruvira, S., Rodríguez-Rodríguez, P., Ramiro-Cortijo, D., Martín-Trueba, M., Martín-Cabrejas, M. A., & Arribas, S. M. (2023). Cocoa shell extract reduces blood pressure in aged hypertensive rats via the cardiovascular upregulation of endothelial nitric oxide synthase and nuclear factor (erythroid-derived 2)-like 2 protein expression. *Antioxidants, 12*, Article 1698. https://doi.org/10.3390/antiox12091698

Sakakibara, T., Sawada, Y., Wang, J., Nagaoka, S., & Yanase, E. (2019). Molecular mechanism by which tea catechins decrease the micellar solubility of cholesterol. *Journal of Agricultural and Food Chemistry, 67*, 7128–7135. https://doi.org/10.1021/acs.jafc.9b02265

de Silva, M. O., Honfoga, J. N. B., deMedeiros, L. L., Madruga, M. S., Bezerra, T. K. A., de Medeiros, L. L., Madruga, M. S., & Bezerra, T. K. A. (2021). Obtaining bioactive compounds from the coffee husk (*Coffea arabica* L.) using different extraction methods. *Molecules, 26*(1), 46. https://doi.org/10.3390/MOLECULES26010046

Singh, M., Thrimawithana, T., Shukla, R., & Adhikari, B. (2020). Managing obesity through natural polyphenols: A review. *Future Foods, 1*, 2. https://doi.org/10.1016/j.fufo.2020.100002

Taladrid, D., Rebollo-Hernanz, M., Martin-Cabrejas, M. A., Moreno-Arribas, M. V., & Bartolomé, B. (2023). Grape pomace as a cardiometabolic health-promoting ingredient: activity in the intestinal environment. *Antioxidants, 12*, 979. https://doi.org/10.3390/antiox12040979

Tan, Y., Kim, J., Cheng, J., Ong, M., Lao, W. G., Jin, X. L., Lin, Y. G., Xiao, L., Zhu, X. Q., & Qu, X. Q. (2017). Green tea polyphenols ameliorate non-alcoholic fatty liver disease through upregulating AMPK activation in high fat fed Zucker fatty rats. *World Journal of Gastroenterology, 23*(21), 3805–3814. https://doi.org/10.3748/wjg.v23.i21.3805

Vásquez-Villanueva, R., Plaza, M., García, M. C., Turner, C., & Marina, M. L. (2019). A sustainable approach for the extraction of cholesterol-lowering compounds from an olive by-product based on CO2-expanded ethyl acetate. *Analytical and Bioanalytical Chemistry, 411*(22), 5885–5896. https://doi.org/10.1007/s00216-019-01970-4

Xu, W., Luo, Y., Yin, J., Huang, M., & Luo, F. (2023). Targeting AMPK signaling by polyphenols: A novel strategy for tackling aging. *Food & Function, 14*, 56. https://doi.org/10.1039/d2fo02688k

Yang, I., Jayaprakasha, G. K., & Patil, B. (2018). *In vitro* digestion with bile acids enhances the bioaccessibility of kale polyphenols. *Food & Function, 9*(2), 1235–1244. https://doi.org/10.1039/c7fo01749a

Yassin Zamanian, M., Sadeghi Ivraghi, M., Khachatryan, L. G., Vadiyan, D. E., Yavarpour Bali, H., Golmohammadi, M., & Mohammad Yassin Zamanian, C. (2023). A review of experimental and clinical studies on the therapeutic effects of pomegranate (Punica granatum) on non-alcoholic fatty liver disease: Focus on oxidative stress and inflammation. *Food Science & Nutrition, 11*, 7485–7503. https://doi.org/10.1002/fsn3.3713

Zhang, R., Zhang, Z., Zhang, H., Decker, E. A., & McClements, D. J. (2015). Influence of emulsifier type on gastrointestinal fate of oil-in-water emulsions containing anionic dietary fiber (pectin). *Food Hydrocolloids, 45*, 175–185. https://doi.org/10.1016/J.FOODHYD.2014.11.020

Zhao, Y., He, Z., Hao, W., Zhu, H., Liu, J., Ma, K. Y., He, W.-S., & Chen, Z.-Y. (2021). Cholesterol-lowering activity of protocatechuic acid is mediated by increasing the excretion of bile acids and modulating gut microbiota and producing short-chain fatty acids. *Food & Function, 12*, 11557. https://doi.org/10.1039/d1fo02906a

Zhou, K., Xia, W., Zhang, C., & Yu, L.(Lucy) (2006). *In vitro* binding of bile acids and triglycerides by selected chitosan preparations and their physico-chemical properties. *LWT - Food Science and Technology, 39*(10), 1087–1092. https://doi.org/10.1016/J.LWT.2005.07.009